

AperTO - Archivio Istituzionale Open Access dell'Università di Torino

**Combined untargeted and targeted fingerprinting with comprehensive two-dimensional chromatography for volatiles and ripening indicators in olive oil**

**This is the author's manuscript**

*Original Citation:*

*Availability:*

This version is available <http://hdl.handle.net/2318/1589438> since 2016-12-01T15:37:20Z

*Published version:*

DOI:10.1016/j.aca.2016.07.005

*Terms of use:*

Open Access

Anyone can freely access the full text of works made available as "Open Access". Works made available under a Creative Commons license can be used according to the terms and conditions of said license. Use of all other works requires consent of the right holder (author or publisher) if not exempted from copyright protection by the applicable law.

(Article begins on next page)

This Accepted Author Manuscript (AAM) is copyrighted and published by Elsevier. It is posted here by agreement between Elsevier and the University of Turin. Changes resulting from the publishing process - such as editing, corrections, structural formatting, and other quality control mechanisms - may not be reflected in this version of the text. The definitive version of the text was subsequently published in *ANALYTICA CHIMICA ACTA*, 936, 2016, 10.1016/j.aca.2016.07.005.

You may download, copy and otherwise use the AAM for non-commercial purposes provided that your license is limited by the following restrictions:

- (1) You may use this AAM for non-commercial purposes only under the terms of the CC-BY-NC-ND license.
- (2) The integrity of the work and identification of the author, copyright owner, and publisher must be preserved in any copy.
- (3) You must attribute this AAM in the following format: Creative Commons BY-NC-ND license (<http://creativecommons.org/licenses/by-nc-nd/4.0/deed.en>), 10.1016/j.aca.2016.07.005

The publisher's version is available at:

<http://linkinghub.elsevier.com/retrieve/pii/S0003267016308261>

When citing, please refer to the published version.

Link to this full text:

<http://hdl.handle.net/2318/1589438>

1 **Combined Untargeted and Targeted fingerprinting with comprehensive**  
2 **two-dimensional chromatography for volatiles and ripening indicators in**  
3 **olive oil**

4  
5  
6  
7  
8  
9  
10 6 Federico Magagna<sup>1§</sup>, Lucia Valverde-Som<sup>2§</sup>, Cristina Ruíz-Samblás<sup>2</sup>, Luis Cuadros-Rodríguez<sup>2</sup>,  
11 7 Stephen E. Reichenbach<sup>3</sup>, Carlo Bicchi<sup>1</sup>, Chiara Cordero<sup>1\*</sup>

12  
13  
14  
15  
16 9 <sup>1</sup> Dipartimento di Scienza e Tecnologia del Farmaco, Università di Torino, Turin, Italy

17 10 <sup>2</sup> Department Analytical Chemistry, Faculty of Science, University of Granada, C/Fuentenueva  
18 11 s/n, 18071, Granada, Spain

19 12 <sup>3</sup> University of Nebraska – Lincoln, Lincoln NE 68588-0115, USA

20  
21  
22  
23  
24  
25 15 § Federico Magagna and Lucia Valverde-Som, listed in alphabetical order, equally contributed  
26 16 to this work

27  
28  
29  
30 19 \* Address for correspondence:

31 20 Prof. Dr. Chiara Cordero - Dipartimento di Scienza e Tecnologia del Farmaco, Università di

32 21 Torino, Via Pietro Giuria 9, I-10125 Torino, Italy – e-mail: [chiara.cordero@unito.it](mailto:chiara.cordero@unito.it);

33 22 Phone: +39 011 6707662; Fax: +39 011 2367662

25 **Abstract**

1  
2  
3  
4  
5  
6  
7  
8  
9  
10  
11  
12  
13  
14  
15  
16  
17  
18  
19  
20  
21  
22  
23  
24  
25  
26  
27  
28  
29  
30  
31  
32  
33  
34  
35  
36  
37  
38  
39  
40  
41  
42  
43  
44  
45  
46  
47  
48  
49  
50  
51  
52  
53  
54  
55  
56  
57  
58  
59  
60  
61  
62  
63  
64  
65

26 Comprehensive two-dimensional gas chromatography (GC×GC) is the most effective  
27 multidimensional separation technique for in-depth investigations of complex samples of  
28 volatiles (VOC) in food. However, each analytical run produces dense, multi-dimensional data,  
29 so elaboration and interpretation of chemical information is challenging.

30 This study exploits recent advances of GC×GC-MS chromatographic fingerprinting to study  
31 VOCs distributions from Extra Virgin Olive Oil (EVOO) samples of a single botanical origin  
32 (Picual), cultivated in well-defined plots in Granada (Spain), and harvested at different  
33 maturation stages. A new integrated work-flow, fully supported by dedicated and automated  
34 software tools, combines *untargeted* and *targeted (UT)* approaches based on peak-region  
35 features to achieve the most inclusive fingerprinting.

36 Combined results from untargeted and targeted methods are consistent, reliable, and  
37 informative on discriminant features (analytes) correlated with optimal ripening of olive fruits  
38 and sensory quality of EVOOs. The great flexibility of the *UT fingerprinting* here adopted  
39 enables retrospective analysis with great confidence and provides data to validate the  
40 transferability of ripening indicators ((*Z*)-3-hexenal, (*Z*)-2-hexenal, (*E*)-2-pentenal, nonanal, 6-  
41 methyl-5-hepten-2-one, octane) to external samples sets. Direct image comparison, based on  
42 *visual* features, also is investigated for quick and effective pair-wise investigations. Its  
43 implementation with reliable metadata generated by *UT fingerprinting* confirms the maturity  
44 of 2D data elaboration tools and makes advanced image processing a real perspective.

45  
46  
47  
48 **Key-words:**

49 Comprehensive two-dimensional gas chromatography-mass spectrometry; untargeted and  
50 targeted fingerprinting ; extra virgin olive oil; olives ripening; retrospective investigations

## 53 1. Introduction

54 Comprehensive two-dimensional gas chromatography (GC×GC) is the most effective  
55 multidimensional separation technique for in-depth investigations of complex samples of  
56 volatiles in food [1]. The combination, in a single analytical platform, of two separation  
57 dimensions with mass spectrometric detection and, when possible, automated sample  
58 preparation, delivers highly efficient sample profiling (detailed analysis of single molecular  
59 entities) and fingerprinting (rapid, high-throughput screening of samples for distinctive  
60 analytical signatures) [2].

61 Each analytical run produces dense, multi-dimensional data, so elaboration and interpretation  
62 of chemical information is a challenging task. In addition, food samples generally have a high-  
63 degree of chemical multidimensionality [3] thus creating highly complex analytical challenges.  
64 In this context, data elaboration strategies should implement smart and productive processes,  
65 preferably with a high degree of automation, to make cross-samples analysis efficient and  
66 informative.

67 Within the existing methodologies for GC×GC data elaboration [4,5], the approach based on  
68 *peak-region* features has been very effective because of its comprehensive and uniform  
69 treatment of information from each sample constituent, both knowns and unknowns. Each  
70 single chemical entity is characterized by its chromatographic and spectrometric parameters  
71 (retention time in both dimensions, detector response, and mass spectral information) and by  
72 its absolute and relative position within the pattern of all detectable constituents. As a  
73 consequence, the 2D peak-retention pattern of a sample is a diagnostic fingerprint,  
74 informative of its composition; and pattern recognition approaches can be successfully applied  
75 to improve effectiveness and productivity in multi-sample data elaboration.

76 Although these concepts are not new for the GC×GC community [6], the full automation of  
77 these procedures and their implementation in commercial software packages has been  
78 achieved only recently. This has limited both routine adoption of the technique for food  
79 analysis and investigative strategies for profiling [2,7].

80 Analysis of olive oil volatiles is a challenging and important problem and GC×GC can yield  
81 deeper knowledge of the composition of this fraction offering new perspectives for quality and  
82 authenticity assessment [8].

83 In spite of the great potential of GC×GC, few studies are available in this field. Vaz Freire et al.  
84 [9] first proposed an image-features approach, or more generally a pattern recognition  
85 methodology, to investigate the characteristic distribution of volatiles from oils. They adopted  
86 open-source image analysis software (Image J, National Institutes of Health) to extract  
87 information from small 2D regions located over the separation space and, by Principal

1  
2  
3  
4  
5  
6  
7  
8  
9  
10  
11  
12  
13  
14  
15  
16  
17  
18  
19  
20  
21  
22  
23  
24  
25  
26  
27  
28  
29  
30  
31  
32  
33  
34  
35  
36  
37  
38  
39  
40  
41  
42  
43  
44  
45  
46  
47  
48  
49  
50  
51  
52  
53  
54  
55  
56  
57  
58  
59  
60  
61  
62  
63  
64  
65

88 Component Analysis (PCA), selected those regions with the highest discrimination potential.  
89 Then, they used targeted profiling to locate known analytes within informative 2D regions.  
90 In 2010, Cajka and co-workers [10] exploited the targeted profiling potential of GC×GC-ToF-MS  
91 and identified 44 analytes able to discriminate samples of different geographical origin and  
92 production year. More recently, Purcaro et al. [8] combined targeted and untargeted analysis  
93 with the goal of a chemical blueprint of olive oil aroma defects. This inter-laboratory study  
94 confirmed the reliability of GC×GC for detailed profiling of olive oil volatile fractions and  
95 introduced an iterative strategy [11,12] to locate sensory-relevant analytes efficiently.

96 This study exploits the most recent advances of GC×GC-MS chromatographic  
97 fingerprinting to study VOC distributions from Extra Virgin Olive Oil (EVOO) samples of a single  
98 botanical origin (Picual), cultivated in well-defined plots in a single region (Granada, Spain), and  
99 harvested at different maturation stages. The principal interest in this application is the quality  
100 characteristics related to optimal ripening of olive fruits [13,14]15,16,17,18,19,20,21] and, as a  
101 consequence, olive oil classification and perceivable sensory quality [22,23]. In particular, this  
102 study proposes an integrated work-flow, fully supported by dedicated software tools, that  
103 performs cross-samples comparisons by contemporarily considering characteristic  
104 distributions (i.e., sample fingerprints) of both known and unknown compounds. This work-  
105 flow integrates both *untargeted* and *targeted (UT) fingerprinting* to realize the most  
106 comprehensive results, and so is termed *UT fingerprinting*. Challenges of retrospective analysis  
107 and immediacy of image fingerprinting also are discussed because of the advantages they offer  
108 in specific investigations.

## 110 **2. Materials and methods**

### 111 **2.1. Reference compounds and solvents**

112 Pure reference standards of  $\alpha$ -thujone, used as Internal Standard (ISTD), at a concentration of  
113 100 mg/L in dibutyl phthalate, and *n*-alkanes (n-C9 to n-C25), used for linear retention index  
114 ( $I_s^T$ ) determination, at a concentration of 100 mg/L in cyclohexane, were supplied by Sigma-  
115 Aldrich (Milan, Italy).  
116 Solvents for *n*-alkanes dilution (toluene and cyclohexane HPLC-grade) and dibutyl phthalate  
117 also were from Sigma-Aldrich.

### 119 **2.2. Olive oil samples**

120 Olive oil samples of *Picual* variety, harvested in 2014, were supplied by "GDR Altiplano de  
121 Granada" (Spain) and were obtained from olives harvested in three different plots in Granada:  
122 "812 *Caniles*" (organic production and drip irrigation); "233-234 *Baza*" (conventional  
123 production and drip irrigation); and "701 *Benamaurel*" (conventional production and drip  
124 irrigation).

125 Each sample was available in duplicate and obtained by mixing olives from at least five  
126 different trees in the same plot to have homogeneous and representative samples. Olives  
127 were harvested at four different ripening stages: November 10-12, 2014; November 24-28,  
128 2014; December 16-17, 2014; and January 12-15, 2015.

129 Samples were analyzed by an accredited laboratory to define quality parameters: acidity (%),  
130 peroxide index (mEq O<sub>2</sub>/kg), and UV absorption. Samples also were submitted to sensory  
131 evaluation by a recognized/official panel [24]. Sample descriptions and acronyms are reported  
132 in **Table 1**, together with quality assessments.

### 134 **2.3. Head-space Solid Phase Micro Extraction sampling devices and conditions**

135 Volatiles were sampled from the headspace (HS) by HS Solid Phase Micro Extraction (HS-  
136 SPME). The sampling protocol was optimized in a previous study [8] and employs a  
137 divinylbenzene/carboxen/polydimethylsiloxane (DVB/CAR/PDMS) 50/30  $\mu$ m, 2 cm length  
138 stableflex fiber from Supelco (Bellefonte, PA, USA).

139 The ISTD ( $\alpha$ -thujone) was pre-loaded onto the fiber before sampling through the standard-in-  
140 fiber procedure. An ISTD solution, 2.0  $\mu$ L, was placed into a 20 mL glass vial and submitted to  
141 HS-SPME at 50°C for 15 minutes (min). The fiber then was exposed to the head-space of olive  
142 oil samples (1.500 g exactly weighted) in 20 mL glass vials, at 50°C for 40 minutes. Last, the  
143 sampled analytes were recovered by introducing the fiber into the S/SL injection port of the

144 GC×GC system at 260°C and thermally desorbed for 5 minutes. Each sample was analyzed in  
145 duplicate.

#### 146 **2.4. Comprehensive two-dimensional gas chromatographic system (GC×GC-MS) set-up and** 147 **analysis conditions**

148 GC×GC analyses were performed on an Agilent 6890 unit coupled to an Agilent 5975C MS  
149 detector (Agilent, Little Falls, DE, USA) operating in EI mode at 70eV. The GC transfer line was  
150 set at 270°C and the MS scan range was 40-240  $m/z$  with a scanning rate of 12,500 amu/s to  
151 obtain a spectra generation frequency of 30 Hz.

152 The system was equipped with a two-stage KT 2004 loop-type thermal modulator (Zoex  
153 Corporation, Houston, TX) cooled with liquid nitrogen and with the hot jet pulse time set at  
154 250 ms with a modulation time of 4 s for all experiments. Fused silica capillary loop dimensions  
155 were 1.0 m long and 0.1 mm inner diameter. The column set was configured as follows: <sup>1</sup>D  
156 SolGel-Wax column (100% polyethylene glycol)(30 m × 0.25 mm  $d_c$ , 0.25  $\mu\text{m}$   $d_f$ ) from SGE  
157 Analytical Science (Ringwood, Australia) coupled with a <sup>2</sup>D OV1701 column (86%  
158 polydimethylsiloxane, 7% phenyl, 7% cyanopropyl) (1 m × 0.1 mm  $d_c$ , 0.10  $\mu\text{m}$   $d_f$ ) from Mega  
159 (Legnano, Milan, Italy).

160 Fiber thermal desorption into the GC injector port was under the following conditions:  
161 split/splitless injector in split mode, split ratio 1:20, injector temperature 250°C. Carrier gas  
162 was helium at a constant flow of 1.8 mL/min. The temperature program was: from 40°C (1  
163 min) to 200°C at 3°C/min and to 250°C at 10°C/min (5 min).

164 The *n*-alkanes liquid sample solution for  $I_s^T$  determination was analyzed under the following  
165 conditions: split/splitless injector in split mode, split ratio 1:50, injector temperature 280°C,  
166 injection volume 1 $\mu\text{L}$ .

167

#### 168 **2.5. Raw data acquisition and GC×GC data handling**

169 Data were acquired by Agilent MSD ChemStation ver E.02.01.00 and processed using GC Image  
170 GC×GC Software version 2.5 (GC Image, LLC Lincoln NE, USA). Statistical analysis was  
171 performed by XLstat (Addinsoft, New York, NY USA) and the PLS Toolbox (Eigenvector Research  
172 Inc., West Eaglerock Drive, Wenatchee, WA, USA) for Matlab<sup>®</sup> software (The Mathworks Inc.,  
173 Natick, MA, USA).

174

#### 175 **2.6 Profiling and advanced fingerprinting work-flow**

176 The bi-dimensional chromatographic data elaboration proposed here was organized in a  
177 sequential work-flow illustrated in **Figure 1**.

178



179 **Insert here Figure 1**

180

181 Untargeted and targeted analyses were performed by applying the *template matching*  
182 fingerprinting strategy, introduced by Reichenbach et al. in 2009 [6]. It uses the patterns of 2D  
183 peaks' metadata (retention times, MS fragmentation patterns, and detector responses) to  
184 establish reliable correspondences between the same chemical entities across multiple  
185 chromatograms. The output of template matching fingerprinting is a data matrix of aligned 2D  
186 peaks and/or peak-regions, together with their related metadata (<sup>1</sup>D and <sup>2</sup>D retention times,  
187 compound names for target analytes, fragmentation pattern, single ions or total ions  
188 response), that can be used for comparative purposes.

189 Targeted analysis (Step 1 of **Figure 1**) focused on about 120 selected compounds, each reliably  
190 identified by matching their EI-MS fragmentation pattern (NIST MS Search algorithm, ver 2.0,  
191 National Institute of Standards and Technology, Gaithersburg, MD, USA, with Direct Matching  
192 threshold 900 and Reverse Matching threshold 950) with those collected in commercial  
193 (NIST2014 and Wiley 7n) and in-house databases. As a further parameter to support reliable  
194 identification, Linear Retention Indices ( $I_s^T$ ) were considered and experimental values  
195 compared with tabulated ones.

196 Untargeted analysis (Step 2 of **Figure 1**) was based on a *peak-regions* features approach [5]  
197 and was performed automatically by GC Image Investigator™ R2.5 (GC-Image LLC, Lincoln NE,  
198 USA). The untargeted analysis included all *peak-regions* above the arbitrarily fixed peak  
199 response threshold of 5,000 counts together with target peaks from Step 1. This approach  
200 [25,26,27,28], briefly described in *Section 3.2*, re-aligned the 48 chromatograms using a set of  
201 *registration peaks*. The resulting data matrix was a 48 × 600 (samples × reliable *peak-regions*).  
202 Response data from aligned 2D *peak-regions* were used for PCA and results cross-compared to  
203 those obtained from target peaks distributions. (See *Section 3.2* for the discussion of results.)

204 *Visual* features fingerprinting, performed as pair-wise image comparison, was the last step of  
205 the study (Step 4 of **Figure 1**) and was rendered with “colorized fuzzy ratio” mode [cite  
206 Hollingsworth et al., JoCA 1105:51, 2006]. The algorithm computes the difference at each data  
207 point between pairs of TICs; a data point is the output of the detector at a point in time. These  
208 differences are mapped into Hue-Intensity-Saturation (HIS) color space to create an image for  
209 visualizing the relative differences between image pairs in the retention-times plane [29]. A  
210 detailed description is provided in *Section 3.4*.

### 211 3. Results and discussion

1 212 The goal of this study was to evaluate the potential of combining Untargeted and  
2 213 Targeted 2D data elaboration approaches based on untargeted *peak-region* features, target  
3 214 peaks, and *visual* features to approach to the most inclusive fingerprinting within EVOO  
4 215 volatiles: the UT fingerprinting strategy. Based on a sampling design focused on a single  
5 216 botanical variety and well-defined geographical locations, VOCs fingerprints were interpreted  
6 217 as a function of ripening stage and oil quality.

7 218 This strategy was inspired by a previous study focused on olive oil aroma defects [8], in which  
8 219 results clearly indicated that the informative potential of GC×GC-MS to delineate specific  
9 220 fingerprints for sensory quality classification of oils. These results showed that a “*strictly*  
10 221 *structured experimental design (considering more variables, such as cultivar, geographical*  
11 222 *origin, etc.)*” would be mandatory to “*robustly and reliably characterize specific markers and*  
12 223 *related characteristics concentration windows*” to support, or even replace, sensory evaluation  
13 224 [8]. In addition, it was clear that larger numbers of “external variables” affecting VOCs pattern  
14 225 reduce the effectiveness of untargeted approaches.

15 226 In the present study, with fewer sample-set variables, and a data elaboration process that  
16 227 combines untargeted and targeted approaches (i.e., *peak-region features, peaks, and visual*  
17 228 *features* methods), we achieve highly effective fingerprinting. The proposed work-flow is  
18 229 comprehensive yet efficient and fully supported by new commercial software. In addition, we  
19 230 validate both the data elaboration strategy and the informative role of some targets by a  
20 231 retrospective investigation on VOCs patterns from EVOO, VOO, and *lampante* oils (LOO)  
21 232 analyzed in previous studies.

22 233 Following this scheme, we first present and discuss results from targeted analysis, focusing on  
23 234 peaks for known informative chemicals and selected VOCs strictly related to the olives’  
24 235 geographical location, ripening stage, and product (oils) quality (presence/absence of sensory  
25 236 defects). Next, untargeted analysis based on peak-regions features, implemented in the  
26 237 second step, is discussed from the perspective of: (a) confirming sample classification results;  
27 238 (b) indicating new potential targets; (c) defining chemical indexes of ripening and quality  
28 239 through the ratio between informative analytes; and (d) validating the role of informative  
29 240 ratios through retrospective elaboration of samples analyzed in previous studies by adopting  
30 241 the *UT* template created on the current sample set. The last part of the study aims at  
31 242 determining if classification based on peak-regions features could be replaced by direct image  
32 243 comparison without losing information about the chemical composition of this fraction. The  
33 244 following paragraphs illustrate the research steps and critically discuss results.

34 245

### 246 3.1 Targeted analysis and samples discrimination

247 The sample set is reported in **Table 1** with their quality parameters, sensory evaluation  
248 results, and commercial classification. Quality metrics (acidity %, peroxide index, UV  
249 absorbance, and organoleptic assessment) indicated that 6 of the 24 samples were not  
250 compliant with *Extra-Virgin* classification [30]. These samples, classified as *Virgin* (VOO) and  
251 *Lampante* (LOO), were from the late ripening stages of the *Baza* and *Benamaurel* plots. This  
252 quality classification was confirmed by replicate sampling (i.e., *Baz\_3\_1/\_2* and *Baz\_4\_1/\_2*;  
253 *Ben\_4\_1/\_2*) and was related to sensory defects revealed by the panel (Median of defects - Md  
254 >0.00). In addition, low-quality samples were connoted by a higher peroxide index and acidity  
255 %.

256 From the available literature [31,32,33,34,35,36,37,38,39], analytes detected in the GC×GC  
257 data were identified by their EI-MS fragmentation pattern and Linear Retention Indices ( $I_s^T$ )  
258 (see section 2.6 for details). Following the work-flow in **Figure 1**, *template-matching*  
259 fingerprinting (see Paragraph 2.6) with 119 target peaks was used to map these informative  
260 chemicals across samples.

261 **Figures 2A-B** shows the pseudocolored GC×GC chromatogram of an EVOO sample from the  
262 *Benamaurel* plot harvested at stage 4 (in January 2015). **Figure 2B** locates the 119 known  
263 target peaks (empty light green circles) linked to the ISTD ( $\alpha$ -tujone black circle) by red lines.

264  
265 **Place here Figures 2A-E**

266  
267 The quali-quantitative distribution of VOCs changed with the harvest stages. The number of  
268 detectable peaks above a Volume threshold of 4,000 (arbitrarily fixed on the Total Ion Current  
269 signal) was about 270-280 at the first stage and reached about 360 at the final stage (data not  
270 shown).

271 The effectiveness of GC×GC, in both peak-capacity and overall chromatographic resolution,  
272 plays a critical role in isolating the information for compounds with similar retention times in  
273 the <sup>1</sup>D dimension. A zoomed region, highlighted in **Fig 2C**, emphasizes the retention area of  
274 highly volatile compounds in which some branched hydrocarbons (eluting later in the <sup>2</sup>D) are  
275 separated along the <sup>2</sup>D from saturated and unsaturated and carbonyl compounds (e.g.,  
276 pentanal, hexanal, (*E*)-2-butenal), and 1-penten-3-one, an odor-active volatile deriving from  
277 linolenic acid degradation), and alcohols (e.g., 1-propanol, 2-butanol, and 2-methyl-2-  
278 propanol).

279 The relative distribution (Normalized 2D Peak Volumes) of the 119 peaks is illustrated as heat-  
280 map in **Supplementary Figure 1 (SF1)**. Columns are ordered left-to-right by <sup>1</sup>D retention indices

281 (polar phase column, 100% polyethylene glycol). The logarithmic colour map is based on 2D-  
282 Peak Volumes divided by ISTD response and is normalized by dividing single values by row  
283 standard deviations.

284 **Table 2** reports the 119 target compounds together with their <sup>1</sup>D and <sup>2</sup>D retention times,  $I^T_s$ ,  
285 sensory descriptors, and correlation with oil defects as reported in reference literature  
286 [31,32,33,34,35,36,37,38,39]. 2D Peak Normalized Volumes (average values of two analytical  
287 replicates) are provided as Supplementary information (**Supplementary Table 1- ST1**).

288 The target analytes distribution (Normalized 2D volumes) was adopted as an informative  
289 fingerprint for possible discrimination of samples within different harvest stages and, in  
290 particular, to locate and validate specific indicators of ripeness, and, when feasible, odor-active  
291 compounds related to sensory quality.

292 Principal Component Analysis (PCA) maps the natural, unsupervised conformation of samples'  
293 groups and sub-groups [40]. **Figure 3A** shows the scores plot on the first two principal  
294 components (F1-F2 plane), based on the 48 × 119 matrix (samples × targets). The variance  
295 from the first principal component (F1) was 30.64% while for the second principal component  
296 (F2) was 10.06%. Autoscaling and mean centering were applied as pre-processing methods,  
297 because baseline correction already was applied for 2D data elaboration by GC Image. The  
298 corresponding loading plots are available as Supplementary information (**Supplementary**  
299 **Figure SF2A**).

300

301 **Insert here Figures 3A-B**

302

303 The PCA shows a clear discrimination between EVOO and VOO (clustered together in the right  
304 side) and *LOO* samples. Additionally, a further sub-classification according to harvesting stage  
305 is evident along F2 and within EVOO samples (see arrow).

306 The samples' structure/classification over the PCA loading plot (see Supplementary  
307 Information **SF2A**) indicates those analytes that are effectively responsible for the  
308 discrimination of *lampante* oils (stage 4 of *Benamaurel* and *Baza*). These analytes include  
309 saturated (e.g., heptanal, octanal, and nonanal) and unsaturated (e.g., (*E*)-2-heptenal)  
310 aldehydes, well-known from the literature to be correlated with specific sensory defects of  
311 olive oils. Moreover, the separation of *lampante* oils is also driven by other compounds,  
312 including some alcohols (e.g., propan-1-ol, 1-octen-3-ol, heptan-1-ol, and octan-1-ol), ketones  
313 (e.g., heptan-2-one and octan-2-one) and esters (e.g., ethyl acetate, ethyl-2-methyl butanoate,  
314 and ethyl-3-methyl butanoate).

1  
2  
3  
4  
5  
6  
7  
8  
9  
10  
11  
12  
13  
14  
15  
16  
17  
18  
19  
20  
21  
22  
23  
24  
25  
26  
27  
28  
29  
30  
31  
32  
33  
34  
35  
36  
37  
38  
39  
40  
41  
42  
43  
44  
45  
46  
47  
48  
49  
50  
51  
52  
53  
54  
55  
56  
57  
58  
59  
60  
61  
62  
63  
64  
65

315 Additional insight on the targets' distribution as a function of harvest time was obtained by  
316 independently processing single subsets of samples by geographical location. In this way, all  
317 variables related to the pedoclimatic conditions and field treatments (organic or conventional)  
318 were excluded, and indications on variables (markers) correlated with ripening stage are more  
319 clearly evidenced. **Figure 3B** shows the score plot for the *Caniles* EVOO subset and the  
320 corresponding loadings plot is provided as Supplementary information (**Supplementary Figure**  
321 **2B -SF2B**).

322 Compounds that contribute most to discriminating harvest stage 1 are: (Z)-2-hexenal,  
323 connoted by a *fruity* note; (Z)-3-hexenal, with *green* odor; and (E,E)-2,4-hexadienal,  
324 contributing a *fresh* note to the overall perception. A group of unsaturated hydrocarbons,  
325 tentatively identified from the literature [41], was found to be distinctive in the discrimination  
326 of the earlier harvest stages (1-2): 3,4-diethyl-1,5-hexadiene (RS+SR), 3,4-diethyl-1,5-  
327 hexadiene (meso), (5Z)-3-Ethyl-1,5-octadiene, (5E)-3-Ethyl-1,5-octadiene, (E,Z)-3,7-decadiene,  
328 (E,E)-3,7-decadiene, and (E)-4,8-Dimethyl-1,3,7-nonatriene. As expected, all these markers  
329 decrease in later ripening stages.

330 Interestingly, but not surprisingly, the evolution of (Z)-2-hexenal and (Z)-3-hexenal, which  
331 provide a *fruity* note (Mf), through time is in accordance with the sensory evaluation of the  
332 panel (as reported in **Table 1**). The relative abundance of these analytes shows a marked  
333 decrease from samples harvested in November (2014) to late January (2015). This observation  
334 is confirmed by data from *Baza* oils where (Z)-3-hexenal falls below method Limit of Detection  
335 (LOD) at stages 3 and 4 consistent with the perception of defects (Md>0.00) leading to their  
336 classification as *lampante* oils, while (Z)-2-hexenal in *Benamaurel* samples was not detected  
337 even at first harvesting time.

338 On the other hand, some other target analytes, for example octane (*sweetly, alcane*), nonanal  
339 (*fatty, waxy*), and 6-methyl-5-hepten-2-one (*pungent, green*), showed an opposite trend by  
340 increasing their relative abundance from stage 1 to the 4. Their presence was not revealed by  
341 the panel, possibly because of their relatively high odor thresholds (octane 940 µg/Kg, nonanal  
342 150 µg/Kg, and 6-methyl-5-hepten-2-one 1000 µg/Kg [22]).

343 These results are consistent with those reported by Aparicio and Morales [19], Raffo et al. [42]  
344 and other researchers [22,43] who hypothesized an increase of autoxidation products (e.g.,  
345 octane and 6-methyl-5-hepten-2-one) accompanied by a decrease of lipooxygenase pathway  
346 products (e.g., (Z)-2-hexenal, (Z)-3-hexenal, and (E,E)-2,4-hexadienal) with later harvest times.  
347 PCA carried out on *Baza* and *Benamaurel* oils (scores and loadings provided as Supplementary  
348 information, **Supplementary Figures 3A and 3B - SF3A and SF3B**) confirms, with some

349 exceptions (e.g., in *Benamaurel* samples), the distribution of the samples and the trend of  
350 these specific chemicals over time from stage 1 to 4.

351

### 352 3.2. Untargeted analysis

353 Untargeted analysis was performed to extend the comparative process to the entire  
354 pattern of detected VOCs. The unsupervised fingerprinting was based on the peak-region  
355 feature approach and implemented by Image Investigator in the GC Image software package.  
356 This data elaboration step was made more informative by considering the 2D peaks included in  
357 the targeted template built within the Step 1 of the work-flow (illustrated in **Figure 1**), thus  
358 preserving all information about known analytes within the fingerprinting.

359 The fully automated procedure of *peak-regions* fingerprinting delineates a small 2D retention-  
360 times window (or *region*) per 2D *peak* over the chromatographic space. Regions are shown in  
361 **Figures 2B** and **2D**, delineated with light blue graphics. In this context, the process approaches  
362 “one-feature-to-one-analyte” selectivity, typical of peak features methods, with all the  
363 advantages of regional features matching [5,27,28]. These advantages includes unambiguous  
364 cross-detection/matching of trace peaks that may be detected in some samples but not in  
365 others and co-eluting analytes that may be resolved in some chromatograms but not in others.

366 The unsupervised procedure is:

- 367 1. Detect and record 2D peaks in individual chromatograms.
- 368 2. Locate *registration* peaks, i.e., peaks that reliably match across all chromatograms  
369 (connoted by red circles in **Figures 2D** and **2E**). This is verified for a sub-group of  
370 targeted peaks.
- 371 3. Align and combine all chromatograms to create a composite chromatogram [5].
- 372 4. Define a pattern of *region* features around every 2D peak detected in the composite  
373 chromatogram.
- 374 5. Create a combined targeted and untargeted template from:
  - 375 a. the registration peaks from Step 2,
  - 376 b. the peak-regions from Step 4, and
  - 377 c. the targeted peaks.

378 The programmed output of the Image Investigator is the template that includes only (a) and  
379 (b). An innovation of this work is the addition of (c) targeted peaks.

380 Once the resulting template, as shown in **Figure 2B** superimposed on the image of the *Baz\_4\_1*  
381 sample - analytical replicate 1, is matched to a target chromatogram, the analysis includes  
382 peak-regions (light blue graphics), targeted peaks (green circles), and registration peaks (red  
383 circles). Feature regions are aligned relative to corresponding peaks, and the characteristics of

384 those features including all metadata (retention times in both chromatographic dimensions,  
385 detector response, relative/absolute intensity, peaks' EI-MS fragmentation pattern, response  
386 factors, etc.) are computed to create a feature vector for the target chromatogram to be  
387 adopted for cross-sample analysis. The final output is a data matrix where peak-regions and  
388 template peaks are cross-aligned within all samples' chromatograms and the response data  
389 are available for further chemometrics.

390 Results based on 180 reliable peak-regions (i.e., those that matched in all-but-one  
391 chromatogram of the set) are shown in **Figure 2B**, and visualized by PCA of **Figure 4A**. They  
392 confirmed what already was evidenced by the known targets distribution: a clear  
393 discrimination of *lampante* oils from VOO and EVOO while maintaining the sub-classification  
394 based on harvesting period. These results account for a total variability of 42%, in line with  
395 previous elaborations.

396 Targeted peak-regions cross-validate the classification based on PCA: (Z)-2-hexenal, (Z)-3-  
397 hexenal, (E,E)-2,4-hexadienal, 1,4-pentadiene, (5Z)-3-ethyl-1,5-octadiene, and (E)-4,8-  
398 dimethyl-1,3,7-nonatriene contribute to the discrimination of stages 1 and 2 against the  
399 others, as obtained in the previous elaboration. Untargeted analysis does not discover  
400 additional informative roles of un-identified features and confirms the coverage of the  
401 targeted peaks.

402 One interesting and positive aspect of these results is the strong accordance between targeted  
403 and untargeted fingerprinting in terms of sample discrimination effectiveness. This result was  
404 not observed when, for example, sampling conditions included too many variables known to  
405 impact the VOCs fingerprint (e.g., cultivars, geographical origin, harvesting period/year,  
406 technological process, bad practices etc.) [8]. In those less-controlled cases, the sensitivity and  
407 effectiveness of untargeted methodologies were lower and targeted analysis gave better  
408 results. In such cases with more experimental variables, much larger numbers of samples may  
409 be required for effective discrimination.

410 Another interesting outcome, in line with previous studies on flavor blueprint [8], is the  
411 accordance between sensory quality scores and samples sub-classes. Because sensory profiles  
412 by descriptive analysis were not available, a direct correlation between odor-active  
413 compounds distribution and sensory quality was not possible. However, positive attributes (Mf  
414 in **Table 1**) had high scores for samples harvested at stages 1 and 2 that rapidly decreased at  
415 stages 3 to 4. Along the same Principal Component (e.g., F2) samples discrimination is in  
416 accordance with both variables (i.e., quality score and ripening stage).

417 Cross-validation of fingerprinting results reinforces and confirms the role played by some  
418 ripening markers responsible for positive attributes (green, fruity and fresh) [22,34]. These

419 compounds appear at stage 1, last up to the stage 2, and then start to decrease. From these  
420 results, and in agreement with quality parameters (**Table 1**), the optimal harvest period to  
421 obtain a product with high sensory quality from *Picual* variety appears to have been November  
422 within stages 1 and 2.

423 Several informative analytes positively and/or negatively correlated with ripening and oil  
424 quality, were therefore selected and their ratio profiled as a function of harvest stages. In  
425 addition, a retrospective analysis on EVOO samples' pattern acquired during a previous study  
426 [8] was performed to verify the reliability and consistency of these indicators.

427

### 428 *3.3 Retrospective analysis and definition of reliable chemical indexes of ripening*

429 Relative ratios (based on 2D Peak Volumes) from the informative chemicals highlighted by the  
430 *UT fingerprinting* were calculated and trends observed along harvest stages.

431 These ratios are functions of sampling parameters (phase ratio,  $\beta$ ; sampling temperature; and  
432 time), but derive from analyses conducted under highly standardized and head-space linearity  
433 conditions. These VOCs fingerprints are therefore informative and replicable, and these ratios  
434 could be transferred to other studies/ batches and considered as chemical indices of ripening.

435 Analytes chosen to discriminate samples at stages 1 and 2 were: (*Z*)-2-Hexenal, (*Z*)-3-Hexenal,  
436 (*E*)-2-Pentenal, and (*E,E*)-2,4-Hexadienal; those chosen that contributed to discriminate the  
437 late harvest stage were: octane, 6-methyl-5-hepten-2-one, and nonanal. Their ratios for the  
438 *Baza* samples set are illustrated by the box-plot graphics in **Figure 5** and correspond to: (*Z*)-3-  
439 Hexenal/6-Methyl-5-hepten-2-one, (*Z*)-3-Hexenal/Nonanal, (*Z*)-2-Hexenal/6-Methyl-5-hepten-  
440 2-one, (*E,E*)-2,4-Hexadienal/6-Methyl-5-hepten-2-one, (*Z*)-3-Hexenal/Octane, (*E*)-2-  
441 Pentenal/Nonanal, (*E*)-2-Pentenal/6-Methyl-5-hepten-2-one, and (*E*)-2-Pentenal/Octane.  
442 Trends were estimated by fittings with exponential, polynomial, or linear functions to  
443 delineate their evolution along harvest stage, resulting functions are reported in **Table 3**. The  
444 accuracy of fittings is as assessed by the determination coefficient ( $R^2$ ).

445

446 **Insert here Figure 5**

447

448 As a general consideration, most of the ratios followed an exponential or second order  
449 polynomial trend with the exception of (*E*)-2-pentenal/octane index whose evolution was  
450 relatively linear. In addition, non-linear trends are connoted by higher informative potential  
451 because of their sudden changes between optimal and non-optimal ripening stages. Notably,  
452 their numeric values decreased one order-of-magnitude between harvest stages where oil  
453 quality changed from EVO to VO or *lampante*.



1  
2  
3  
4  
5  
6  
7  
8  
9  
10  
11  
12  
13  
14  
15  
16  
17  
18  
19  
20  
21  
22  
23  
24  
25  
26  
27  
28  
29  
30  
31  
32  
33  
34  
35  
36  
37  
38  
39  
40  
41  
42  
43  
44  
45  
46  
47  
48  
49  
50  
51  
52  
53  
54  
55  
56  
57  
58  
59  
60  
61  
62  
63  
64  
65

454 The usefulness of such ratios also might be evaluated from a wider perspective where, for  
455 example, VOCs fingerprints are adopted for quality classification of EVO oils. Within selected  
456 volatiles produced during the climacteric stage of ripening [22], (*Z*)-3-hexenal is a product of  
457 the lipoxygenase pathway and, in EVO and VO oils, it contributes to the fresh aroma  
458 perception thanks to its relatively low odor threshold [20,21,34,37]. This compound is also a  
459 cultivar-specific marker for the *Picual* variety [34], as is 6-methyl-5-hepten-2-one that, as a  
460 counterpart, is connoted by a negative odor perception and an incremental trend along  
461 ripening stages. Nonanal provides information about oxidation state as well as octane  
462 [36,37,44,45].

463 To evaluate the consistency and the transferability of this approach for informative chemical  
464 indexes, a retrospective analysis was attempted by re-processing chromatograms from a  
465 previous study [8]. Samples consisted of EVOO from different botanical/geographical origins  
466 and technological processes and from olives harvested in 2013. They were analyzed previously,  
467 in the authors' laboratory, with the same nominal HS-SPME sampling protocol and GC×GC-MS  
468 conditions. Details are reported in **Table 1**.

469 The peak-regions template created in this study (and shown in **Figure 6A** with the *Can\_1\_2*  
470 sample) was matched to these older, GC×GC chromatograms (as shown in **Figure 6B** with the  
471 EVOO oil from Sicily PDO Monti Iblei) after a supervised transformation of the template to  
472 compensate for non-linear retention times differences in both dimensions [46].

473  
474 **Insert here Figures 6A-B**

475  
476 These chromatographic inconsistencies are not infrequent because, in a time frame of two  
477 years, column sets were replaced and/or columns have altered retention behaviour (in  
478 particular the 1D PEG polar phase) producing minimal, but not negligible, pattern alterations.  
479 However, thanks to the specificity of the matching methods, 2D peaks that positively match  
480 are just those with EI-MS fragmentation pattern similarity above 700 (direct match) or 900  
481 (reverse match). Cross-aligned results are in consequence reliable and consistent, making  
482 possible retrospective investigations.

483 Ratios between informative markers for the EVOO samples from *Baza*, *Caniles*, and  
484 *Benamaurel*, plus five samples from the previous study (R-EVOO from 1 to 5), were analyzed by  
485 PCA and the results are shown in **Figure 4B**. The discrimination power of the first two PCs  
486 reaches 94%, confirming the informative power of the combination of variables. *Picual*  
487 samples (*Baz*, *Can* and *Ben*) are clustered together, with the exception of the *Benamaurel*  
488 EVOO at the earliest harvest stage, whereas along F2, there is evident discrimination for

1  
2  
3  
4  
5  
6  
7  
8  
9  
10  
11  
12  
13  
14  
15  
16  
17  
18  
19  
20  
21  
22  
23  
24  
25  
26  
27  
28  
29  
30  
31  
32  
33  
34  
35  
36  
37  
38  
39  
40  
41  
42  
43  
44  
45  
46  
47  
48  
49  
50  
51  
52  
53  
54  
55  
56  
57  
58  
59  
60  
61  
62  
63  
64  
65

489 ripening stage. On the other hand, R-EVOO samples clustered together close to stages 2 and 3,  
490 with the only exception of R-EVOO 2 PDO (Monti Iblei Sicily, Italy), which showed a very high  
491 value for (Z)-3-Hexenal/6-Methyl-5-hepten-2-one because of the high abundance of (Z)-3-  
492 Hexenal (which accounted for 12% of Total Volume). The corresponding loading plot for  
493 informative ratios is provided as Supplementary information **Supplementary Figure 4B - SF4B**.  
494 The proposed ratios are consistent within Picual variety, but to be considered as general  
495 indices for ripening classification their reliability should be verified and validated by analyzing  
496 samples from different harvest years and location, and their transferability to other botanical  
497 origins and geographical locations should be investigated ex-novo by screening samples after a  
498 rigorous sampling design.

### 500 *3.4 Fingerprinting by image features approach*

501 The last part of this study focuses on a fingerprinting approach based on *visual*  
502 features and it is suitable for rapid and effective pair-wise pattern comparisons. The approach  
503 is one of the earliest introduced in GC×GC data elaboration [5], and is still adopted when  
504 distinctive patterns have to be compared on an untargeted basis to immediately reveal  
505 compositional differences.

506 Previous studies demonstrated the potentials of this simple and intuitive approach by  
507 exploring the volatile fraction of roasted coffee and juniper [47], volatiles emitted from  
508 *Chrysolina herbacea* bugs fed by *Mentha* spp. leaves [48], and primary metabolites distribution  
509 in mice urine after dietary manipulation [26]. The same approach was used iteratively, by cross  
510 matching sample pairs, to reveal a chemical blueprint of odor active compounds responsible of  
511 sensory defects [8].

512 In this application, where VOCs variations are mainly related to harvest/ripening stage, the  
513 visual approach would be effective to immediately highlight 2D peaks and/or analytes that  
514 have significantly different relative distributions between sample pairs. In addition, by  
515 comparing samples within the same production plot, the effect of fruit maturation is magnified  
516 while keeping constant the effect of local pedoclimatic changes.

517 This fully automated approach, namely Image Comparison (GC Image v2.5b), if implemented  
518 with peak-regions fingerprinting template, provides immediate information about targeted or  
519 untargeted peak-regions variations between pair-wise compared samples.

520 The example here illustrated refers to a *Benamaurel* oil sample obtained at stage 1 (averaged  
521 normalized image from *Ben\_1\_1* and *Ben\_1\_2*) arbitrarily considered as the *analyzed* image  
522 versus the stage 4 samples (averaged normalized image from *Ben\_4\_1* and *Ben\_4\_2*) arbitrarily  
523 considered as the *reference* image.

524 **Figure 7** shows the image comparison results between the average image of harvest stage 1  
525 (**Fig. 7A**) and stage 4 (**Fig. 7B**) obtained by averaging the 2D chromatograms from two replicate  
526 locations and two analytical runs. The resulting image (**Fig. 7C**) is rendered as “colorized fuzzy  
527 ratio” that uses the Hue-Intensity-Saturation (HIS) color space to color each pixel in the  
528 retention-times plane. The algorithm computes the difference at each data point between  
529 aligned pair-wise images. If a pixel is colored green, then the difference is positive, indicating a  
530 larger detector response in the *analyzed* image (*Ben\_1\_1 and Ben\_1\_2*). If a pixel is colored  
531 red, then the difference is negative, indicating a larger detector response in the *reference*  
532 image (*Ben\_4\_1 and Ben\_4\_2*). Brightness depends on the magnitude of the difference, and  
533 so white saturation indicates pixels at which peaks have detector responses that are nearly  
534 equal in the analyzed and reference images.

535

536 **Insert here Figures 7A-C**

537

538 Because the 2D chromatograms submitted to the image comparison were already pre-  
539 processed by *peak-region* fingerprinting, results are implemented with the information about  
540 2D peaks' identity (if known) or unique identification numbering (#) for unknowns.

541 Results of *visual* features fingerprinting are intuitive and promptly give information on  
542 discriminant peaks. Green colored regions in the upper part of the 2D plot at lower <sup>1</sup>D  
543 retention correspond to unsaturated alkanes [41] (#ID 10, 11, 15, 17, 21), unsaturated  
544 aldehydes (#30 (E)-2-Pentenal, #32 (Z)-3-Hexenal, #34 (E)-3-Hexenal, #42 (Z)-2-Hexenal, #44 (E)-  
545 2-Hexenal, #71 (E,Z)-2,4-Hexadienal, and #73 (E,E)-2,4-Hexadienal), whereas red areas  
546 corresponds to limonene (#41), short chain fatty acids (#107 hexanoic, #115 octanoic and #117  
547 nonanoic acid), linear saturated aldehydes (#12 pentanal, #54 octanal and #70 decanal), and  
548 some ketones, such as 6-methyl-5-hepten-2-one (#63).

549

#### 550 **4. Conclusions**

551 This study evidences and emphasizes the potentials of fingerprinting based on GC×GC-  
552 MS separations and highlights the synergism between untargeted and targeted methodologies  
553 to investigate complex fractions of volatiles in depth. Their combination enables to achieve the  
554 most inclusive/comprehensive fingerprinting (*UT fingerprinting*) and if compared to previous  
555 studies, the degree of automation implemented in the data elaboration work-flow is  
556 promising. Experimental results on EVOO volatiles definitely confirm the maturity of available  
557 software tools to exploit dense and multi-level data set effectively.

1  
2  
3  
4  
5  
6  
7  
8  
9  
10  
11  
12  
13  
14  
15  
16  
17  
18  
19  
20  
21  
22  
23  
24  
25  
26  
27  
28  
29  
30  
31  
32  
33  
34  
35  
36  
37  
38  
39  
40  
41  
42  
43  
44  
45  
46  
47  
48  
49  
50  
51  
52  
53  
54  
55  
56  
57  
58  
59  
60  
61  
62  
63  
64  
65

558 The consistency and reliability of cross-sample analysis results in revealing  
559 informative/discriminant features is confirmed by matching results from different approaches,  
560 and is of interest in this challenging application field where accurate fingerprinting can be very  
561 useful: (a) to support studies aimed at improving product quality; (b) to define a distinctive  
562 chemical fingerprint to discriminate samples of a certain botanical/geographical origin; and (c)  
563 to re-investigate, on a retrospective projection, samples in light of new informative features.  
564

565 **Acknowledgments**

1 566 The authors are grateful to “GDR Altiplano de Granada” (Spain) for olives samples.  
2

3 567 The research was carried out thanks to the support "International mobility program for young  
4  
5 568 researchers (PhD)” by University of Granada and CEI BioTic Granada.  
6

7 569

8 570 Note: S. E. Reichenbach has a financial interest in GC Image, LLC.  
9

10 571  
11  
12  
13  
14  
15  
16  
17  
18  
19  
20  
21  
22  
23  
24  
25  
26  
27  
28  
29  
30  
31  
32  
33  
34  
35  
36  
37  
38  
39  
40  
41  
42  
43  
44  
45  
46  
47  
48  
49  
50  
51  
52  
53  
54  
55  
56  
57  
58  
59  
60  
61  
62  
63  
64  
65

572 **Figure Captions:**

1  
2 573 **Figure 1:** Two-dimensional chromatographic data elaboration work-flow.  
3  
4 574

5 575 **Figures 2A-E:** (2A) Pseudocolored GC×GC chromatogram of *Ben\_4\_1* harvested at stage 4 (in  
6 January 2015). (2B) Position of the 119 known target peaks (empty light green circles) linked to  
7 the ISTD ( $\alpha$ -tujone black circle) by red lines. (2C) Retention area of highly volatile compounds  
8 referred to the white rectangle of Fig. 2A. (2D) Peak-regions delineated by light blue graphics  
9 together with targeted peaks (empty light blue circles). (2E) Results of comprehensive  
10 template matching for peak-regions, target peaks (green circles) and registration peaks (red  
11 circles). For details see text.  
12  
13  
14  
15  
16  
17

18 582

19 583 **Figures 3A-B:** PCA results. (3A) Scores plot on the first two principal components (F1-F2 plane),  
20 based on targets distribution across all samples (48 × 119 matrix - samples × targets). (3B)  
21 Scores plot the first two principal components (F1-F2 plane) based on targets distribution  
22 across *Caniles* EVOO subset.  
23  
24  
25  
26

27 587

28 588 **Figures 4A-B:** PCA results. (4A) Scores plot on the first two principal components (F1-F2 plane),  
29 based on reliable *peak-regions* distribution across all samples (48 × 180 matrix - samples ×  
30 reliable *peak-regions*). (3B) Scores plot the first two principal components (F1-F2 plane) based  
31 on informative ratios between ripening markers. For details see text.  
32  
33  
34  
35

36 592

37 593 **Figure 5:** Box-plot graphics showing the evolution of different informative ratios between  
38 ripening markers along harvest stages for Baza plot samples.  
39  
40

41 595

42 596 **Figures 6A-B:** (6A) 2D chromatogram of *Can\_1\_2* sample together with the reliable peak-  
43 regions template. (6B) 2D chromatogram of *R-EVOO 2* sample (PDO Monti Iblei - Sicily Italy)  
44 together with the reliable peak-regions template tranformed and adapted with a supervised  
45 approach.  
46  
47  
48

49 600

50  
51 601 **Figures 7A-C:** (7A) Averaged 2D-chromatogram of *Benamaurel* oil samples (field replicates and  
52 analytical replicates) obtained at stage 1 and (7B) at stage 4. (7C) Image comparison results  
53 between average image of harvest stage 1 (7A) and stage 4 (7B). The resulting image is  
54 rendered as “colorized fuzzy ratio”. Analytes that varied between stages are listed together  
55 with their unique ID numbering (ref. Table 2).  
56  
57  
58  
59  
60

60 606

1  
2  
3  
4  
5  
6  
7  
8  
9  
10  
11  
12  
13  
14  
15  
16  
17  
18  
19  
20  
21  
22  
23  
24  
25  
26  
27  
28  
29  
30  
31  
32  
33  
34  
35  
36  
37  
38  
39  
40  
41  
42  
43  
44  
45  
46  
47  
48  
49  
50  
51  
52  
53  
54  
55  
56  
57  
58  
59  
60  
61  
62  
63  
64  
65

607 **Table Captions:**

608

609 **Table 1:** List of analyzed samples together with plot denomination, field replicate, harvest  
610 stage, acronym, quality parameters according to COMMISSION REGULATION (EEC) No 2568/91  
611 of 11 July 1991, sensory evaluation results, and commercial classification.

612

613 **Table 2:** List of the 119 target analytes together with <sup>1</sup>D and <sup>2</sup>D retention times,  $I_s^T$  and sensory  
614 descriptors as reported in reference literature [31,32,33,34,35,36,37,38,39]. The 2D Peak  
615 Volume data is provided as Supplementary information in **Supplementary Table 1 - ST1**.

616

617 **Table 3:** Ripening informative markers evolution trends along harvest stages. The quality of  
618 fittings is referred as Coefficient of Determination ( $R^2$ ).

619

- [1] P.Q. Tranchida, P. Donato, F. Cacciola, M. Beccaria, P. Dugo, L. Mondello, Potential of comprehensive chromatography in food analysis. *TrAC Trends Anal Chem* 52 (2013) 186-205
- [2] C. Cordero, J. Kiefl, P. Schieberle, S.E. Reichenbach, C. Bicchi, Comprehensive two-dimensional gas chromatography and food sensory properties: potential and challenges. *Anal. Bioanal. Chem.* 407 (2015) 169-191.
- [3] C. Giddings, Sample dimensionality: a predictor of order-disorder in component peak distribution in multidimensional separation, *J. Chromatogr. A* 703 (1995) 3-15
- [4] Z. Zeng, J. Li, H.M. Hugel, G. Xu, P.J. Marriott, Interpretation of comprehensive two-dimensional gas chromatography data using advanced chemometrics. *TrAC Trends Anal Chem* 53 (2014) 150-66
- [5] S.E. Reichenbach, X. Tian, C. Cordero, Q. Tao, Features for non-targeted cross-sample analysis with comprehensive two-dimensional chromatography, *J. Chromatogr. A* 1226 (2012) 140-148
- [6] S.E. Reichenbach, P.W. Carr, D.R. Stoll, Q. Tao, Smart templates for peak pattern matching with comprehensive two-dimensional liquid chromatography. *J. Chromatogr. A* 1216 (2009). 3458-3466.
- [7] P.Q. Tranchida, G. Purcaro, M. Maimone, L. Mondello, Impact of comprehensive two-dimensional gas chromatography with mass spectrometry on food analysis. *J Sep Sci* 39 (2016) 149-61
- [8] G. Purcaro, C. Cordero, E. Liberto, C. Bicchi, L. S. Conte, Toward a definition of blueprint of virgin olive oil by comprehensive two-dimensional gas chromatography. *J. Chromatogr. A*, 1334 (2015) 101-111.
- [9] L.T. Vaz-Freire, M.D.R.G. da Silva, A.M.C. Freitas, Comprehensive two-dimensional gas chromatography for fingerprint pattern recognition in olive oils produced by two different techniques in portuguese olive varieties galega vulgar, cobrançosa e carrasquenha. *Anal Chim Acta* 633 (2009) 263-70.
- [10] T. Cajka, K. Riddellova, E. Klimankova, M. Cerna, F. Pudil, J. Hajslova, Traceability of olive oil based on volatiles pattern and multivariate analysis. *Food Chem* 121 (2010) 282-9
- [11] C. Cordero, E. Liberto, C. Bicchi, P. Rubiolo, S.E. Reichenbach, X. Tian, Q. Tao, Targeted and non-targeted approaches for complex natural sample profiling by GC×GC -qMS. *J Chromatogr Sci* 48 (2010) 251-61.
- [12] C. Cordero, E. Liberto, C. Bicchi, P. Rubiolo, P. Schieberle, S.E. Reichenbach, Q. Tao, Profiling food volatiles by comprehensive two-dimensional gas chromatography coupled with mass spectrometry: Advanced fingerprinting approaches for comparative analysis of the volatile fraction of roasted hazelnuts (*Corylus avellana* L.) from different origins. *J Chromatogr A* 1217 (2010) 5848-58.
- [13] M.N. Franco, J. Sánchez, C. De Miguel, M. Martínez, D. Martín-Vertedor. Influence of the fruit's ripeness on virgin olive oil quality. *J. Oleo Sci.*, 64 (3) (2015), 263-273.
- [14] L.C. Matos, S.C. Cunha, J.S. Amaral, J.A. Pereira, P.B. Andrade, R.M. Seabra, B.P.P. Oliveira, Chemometric characterization of three varietal olive oils (Cvs. Cobrançosa, Madural and Verdeal Transmontana) extracted from olives with different maturation indices. *Food Chem.*, 102 (2007). 406-414.
- [15] L. Martínez Nieto, G. Hodaifa, J.L. Lozano Peña, Changes in phenolic compounds and rancimat stability of olive oils from varieties of olives at stages of ripeness. *J Sci Food Agric.* 90, (2010) 2393-2398.
- [16] T.Gallina-Toschi, L. Cerretani, A. Bendini, M. Bonoli-Carbognin, G. Lercker, Oxidative stability and phenolic content of virgin olive oil: an analytical approach by traditional and high resolution techniques. *J. Sep. Sci.* 28 (2005). 859-870.



- 
- 1 [17] L. Nasini, P. Proietti, Olive harvesting. In: Peri C. (ed). The extra-virgin olive oil handbook.  
2 John Wiley Blackwell, Chichester (UK) (2014). pp. 89-105.
- 3 [18] M.N. Franco, J. Sánchez, C. De Miguel, M. Martínez, D. Martín-Vertedor, Influence of the  
4 fruit's ripeness on virgin olive oil quality. *J. Oleo Sci.*, 64 (3) (2015). 263-273.
- 5 [19] R. Aparicio, M.T. Morales, Characterization of olive ripeness by green aroma compounds  
6 of virgin olive oil. *J Agric Food Chem*, 46 (1998) 1116-1122.
- 7 [20] Morales M.T., Aparicio R., Calvente J.J.. Influence of olive ripeness on the concentration of  
8 green aroma compounds in virgin olive oil. *Flav. Frag. J.*, 11 (1996) 171-178.
- 9 [21] R. Aparicio, G. Luna, Characterisation of monovarietal virgin olive oils. *Eur. J. Lipid Sci.*  
10 *Technol.* 104, (2002). 614-627.
- 11 [22] C.M. Kalua, M.S. Allen, Jr. Bedgood, A.G. Bishop, P.D. Prenzler, K. Robards, Olive oil volatile  
12 compounds, flavour development and quality: A critical review. *Food. Chem.* 100 (2007) 273-  
13 286.
- 14 [23] A.M. Inarejos-García, M. Santacatterina, M.D. Salvador, G. Fregapane, S. Gómez-Alonso,  
15 PDO virgin olive oil quality-Minor components and organoleptic evaluation. *Food Res. Int.* 43  
16 (2010). 2138-2146.
- 17 [24] Regulation EU No 1348/2013 on the characteristics of olive oil and olive-residue oil and on  
18 the relevant methods of analysis
- 19 [25] S.E. Reichenbach, D.W. Rempe, Q. Tao, D. Bressanello, E. Liberto, C. Bicchi, S. Balducci, C.  
20 Cordero, Alignment for comprehensive two-dimensional gas chromatography with dual  
21 secondary columns and detectors. *Anal Chem* ;87(19) (2015) 10056-63
- 22 [26] D. Bressanello, E. Liberto, M. Collino, S.E. Reichenbach, E. Benetti, F. Chiazza, C. Bicchi, C.  
23 Cordero, Urinary metabolic fingerprinting of mice with diet-induced metabolic derangements  
24 by parallel dual secondary column-dual detection two-dimensional comprehensive gas  
25 chromatography. *J Chromatogr A* ;1361 (2014) 265-76.
- 26 [27] S.E. Reichenbach, X. Tian, A.A. Boateng, C.A. Mullen, C. Cordero, Q. Tao, Reliable peak  
27 selection for multisample analysis with comprehensive two-dimensional chromatography. *Anal*  
28 *Chem* 85(10) (2013)4974-81.
- 29 [28] S.E. Reichenbach, X. Tian, Q. Tao, E.B. Ledford, Jr., Z. Wu, O. Fiehn. Informatics for cross-  
30 sample analysis with comprehensive two-dimensional gas chromatography and high-resolution  
31 mass spectrometry (GCxGC-HRMS). *Talanta* 83(4) (2011) 1279-88.
- 32 [29] B. Hollingsworth, S. Reichenbach, Q. Tao, and A. Visvanathan. "Comparative Visualization  
33 for Comprehensive Two-Dimensional Gas Chromatography." *Journal of Chromatography A*,  
34 1105(1-2):51-58, 2006
- 35 [30] COMMISSION REGULATION (EEC) No 2568/91 of 11 July 1991 on the characteristics of  
36 olive oil and olive-residue oil and on the relevant methods of analysis and successive  
37 emendments.
- 38 [31] K. Kotsiou, M. Tasioula-Margari, Changes occurring in the volatile composition of Greek  
39 virgin olive oils during storage: oil variety influences stability. *Eur. J. Lipid Sci. Technol.* 117  
40 (2015). 514-522.
- 41 [32] I. Romero, D. L. García-González, R. Aparicio-Ruiz, M. T. Morales, Validation of SPME-  
42 GCMS method for the analysis of virgin olive oils volatiles responsible for sensory defects.  
43 *Talanta*, 134 (2015) 394-401.
- 44 [33] L. Cerretani, M. Desamparados Salvador, A. Bendini, G. Fregapane, Relationship between  
45 sensory evaluation performed by Italian and Spanish official panels and volatile and phenolic  
46 profiles of virgin olive oils. *Chem. Percept.* 1 (2008) 258-267.
- 47 [34] G. Luna, M. T. Morales, R. Aparicio, Characterisation of 39 varietal virgin olive oils by their  
48 volatile composition. *Food Chem.*, 98 (2006) 243-252.
- 49 [35] R. Iraqi, C. Vermeulen, A. Benzekri, A. Bouseta, S. Collin, Screening for key odorants in  
50 Moroccan green olives by gas chromatography-olfatometry/aroma extract dilution analysis. *J.*  
51 *Agric. Food Chem.*, 53 (2005) 1179-1184.
- 52  
53  
54  
55  
56  
57  
58  
59  
60  
61  
62  
63  
64  
65

- 
- 1 [36] M. T.Morales, G. Luna, R. Aparicio, Comparative study of virgin olive oil sensory defects.  
2 Food Chem., 91 (2005) 293-301.
- 3 [37] Reiners J., Grosch W. Odorants of virgin olive oils with different flavor profiles. J. Agric.  
4 Food Chem. 46 (1998) 2754-2763.
- 5 [38] M. Rychlik, P. Schieberle, W. Grosch (1998). Compilation of odor thersholds, odor qualities  
6 and retention indeces of key food odorants. Deutsche Forschungsanstalt für  
7 Lebensmittelchemie and Institut für Lebensmittelchemie der Technischen Universität  
8 München. Garching, Germany.
- 9 [39] <http://www.flavornet.org/flavornet.html> [Check: 02 May 2016].
- 10 [40] R. Leardi (2003). Chemometrics in data analysis. In: Lees M. (ed). Food authenticity and  
11 traceability. Ed. Woodhead, Cambridge.
- 12 [41] F. Angerosa, L. Camera, N. D'Alessandro, G. Mellerio Characterization of seven new  
13 hydrocarbon compounds present in the aroma of virgin olive oils, J. Agric. Fodd Chem. 46 (2)  
14 (1998) 648-653
- 15 [42] A. Raffo, R. Bucci, A. D'Aloise, G. Pastore Combined effects of reduced malaxation oxygen  
16 levels and storage time on extra-virgin olive oil volatiles investigated by a novel chemometric  
17 approach. Food Chem. 182 (2015) 257-267.
- 18 [43] M.D.R.Gomes da Silva, A.M. Costa Freitas, M.J.B. Cabrita, Garcia Raquel. Olive oil  
19 composition: volatile compounds, in: Boskou D. Olive oil-constituents, quality, health  
20 properties and bioconversions, Rijeka, Croatia, 2011, pp. 17-46.
- 21 [44] V.Messina, A. Sancho, N. Walsöe de Reça Monitoring odour of heated extra-virgin olive  
22 oils from Arbequina and Manzanilla cultivars using an electronic nose. Eur. J. Lipid Sci.  
23 Technol. 117 (2015) 1-6.
- 24 [45] A. Kanavouras, P. Hernandez-Münoz, F. Coutelieris, S. Selke Oxidation-derived flavor  
25 compounds as quality indicators for packaged olive oil. J. Am. Oil Chem. Soc., 81, (2004) 251-  
26 257.
- 27 [46] GC Image, LLC. GC Image GCxGC Edition Users' Guide, R2.6, 2016
- 28 [47] C. Cordero, E. Liberto, C. Bicchi, P. Rubiolo, S.E. Reichenbach, X. Tian, Q. Tao. Targeted and  
29 non-targeted approaches for complex natural sample profiling by GCxGC-qMS. J. Chromatogr.  
30 Sci. 48 (2010) 251.
- 31 [48] C. Cordero, S.A. Zebelo, G. Gnavi, A. Griglione, C. Bicchi, M.E. Maffei, P. Rubiolo, HS-  
32 SPME-GCxGC-qMS volatile metabolite profiling of Chrysolina herbacea frass and Mentha spp.  
33 leaves. Analytical and Bioanalytical Chemistry 402 (2012) 1941-1952
- 34  
35  
36  
37  
38  
39  
40  
41  
42  
43  
44  
45  
46  
47  
48  
49  
50  
51  
52  
53  
54  
55  
56  
57  
58  
59  
60  
61  
62  
63  
64  
65

Figure 1

Click here to download Figure: Figure 1.pptx

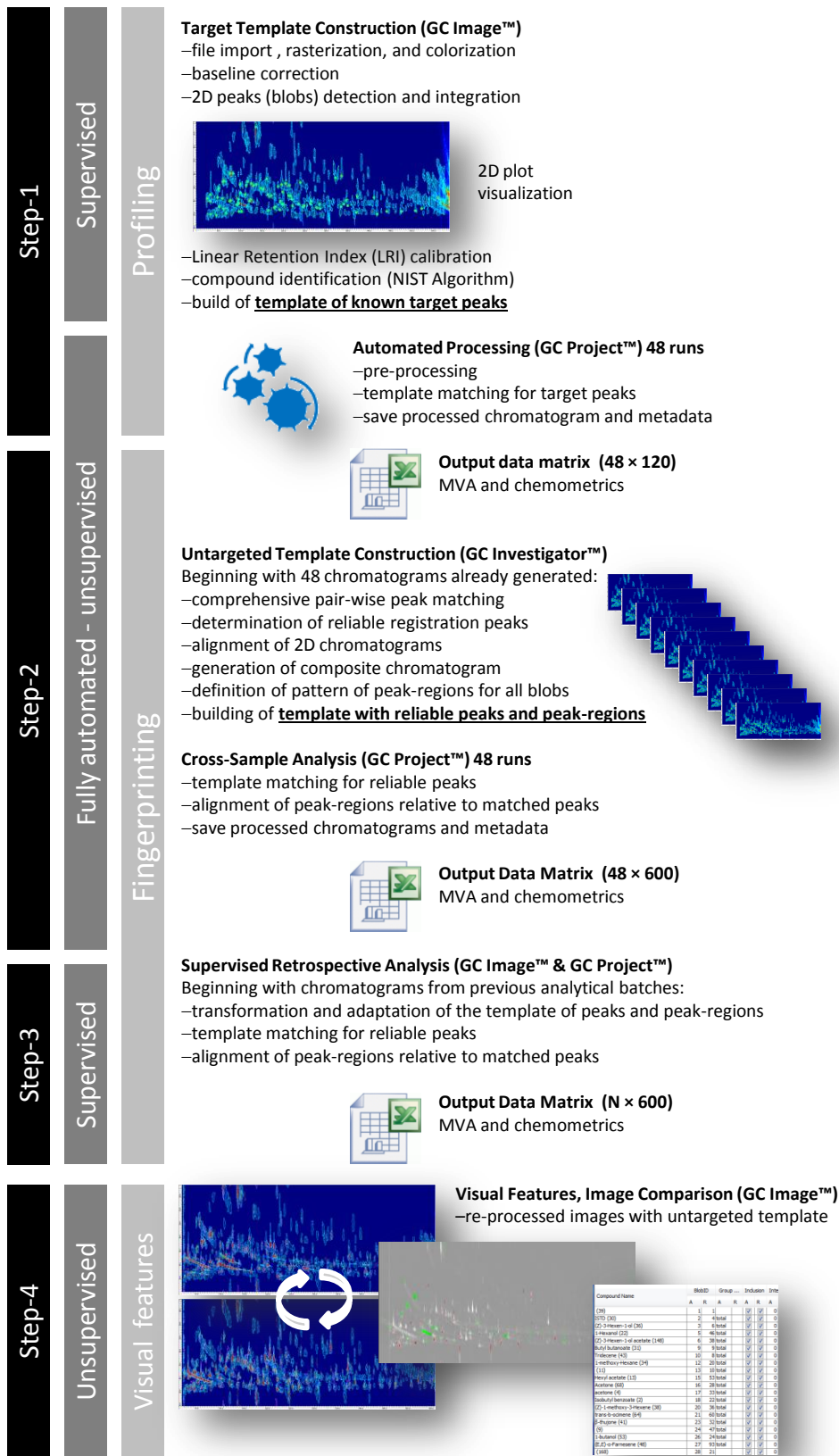


Figure 2 new

[Click here to download Figure: Figure 2rev.pptx](#)

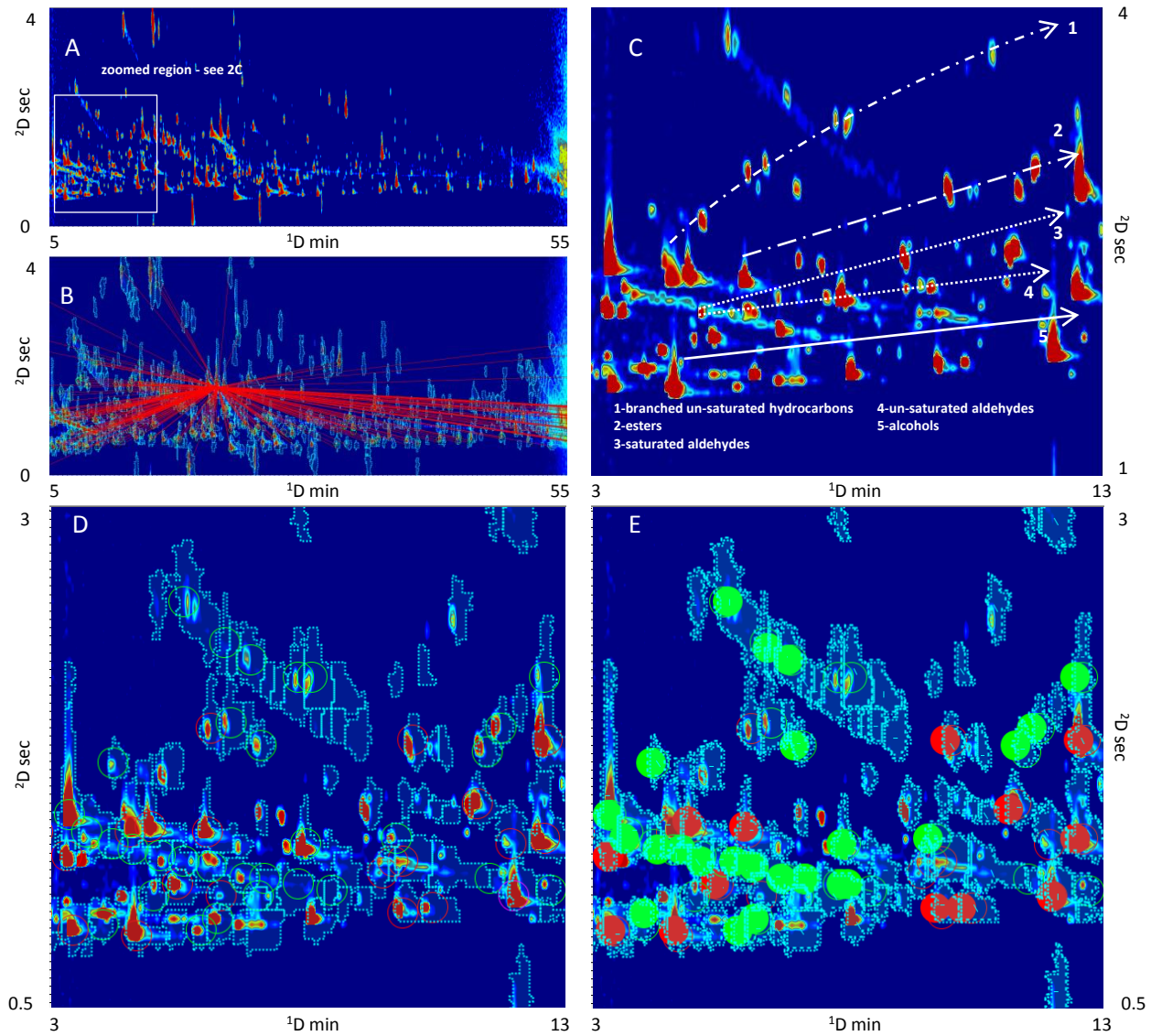


Figure 3

[Click here to download Figure: Figure 3.pptx](#)

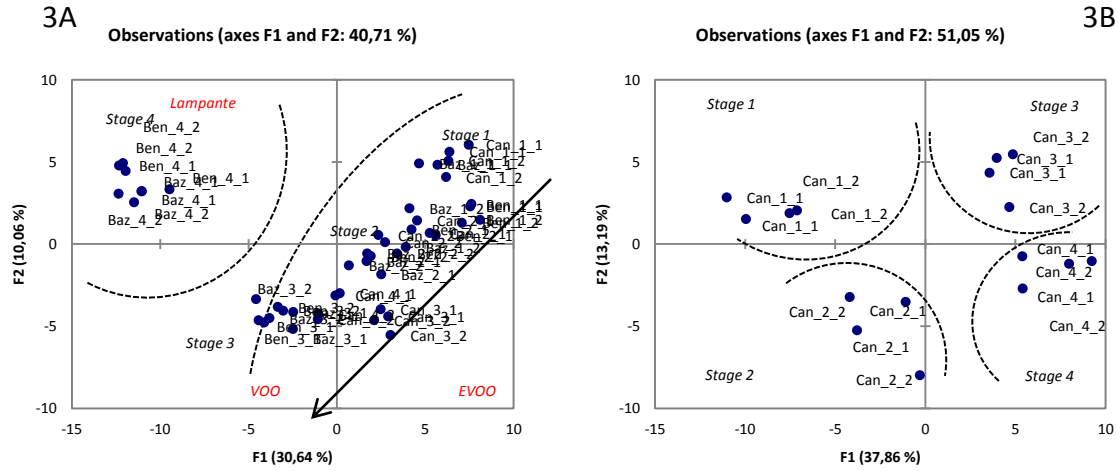
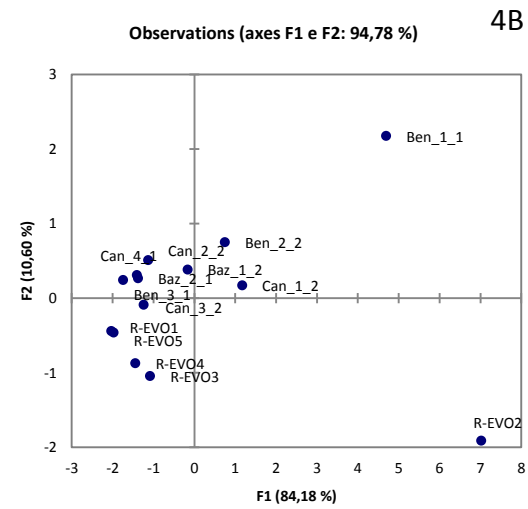
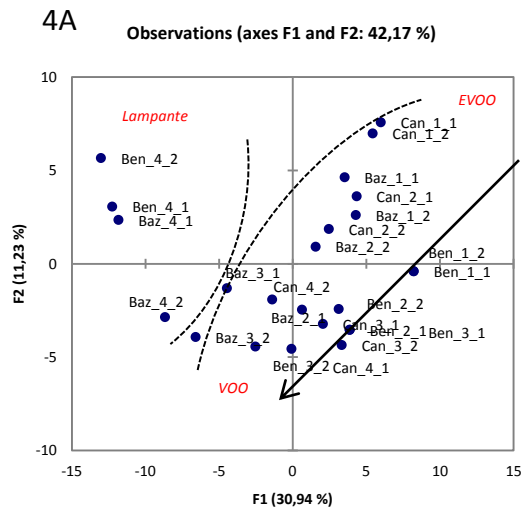
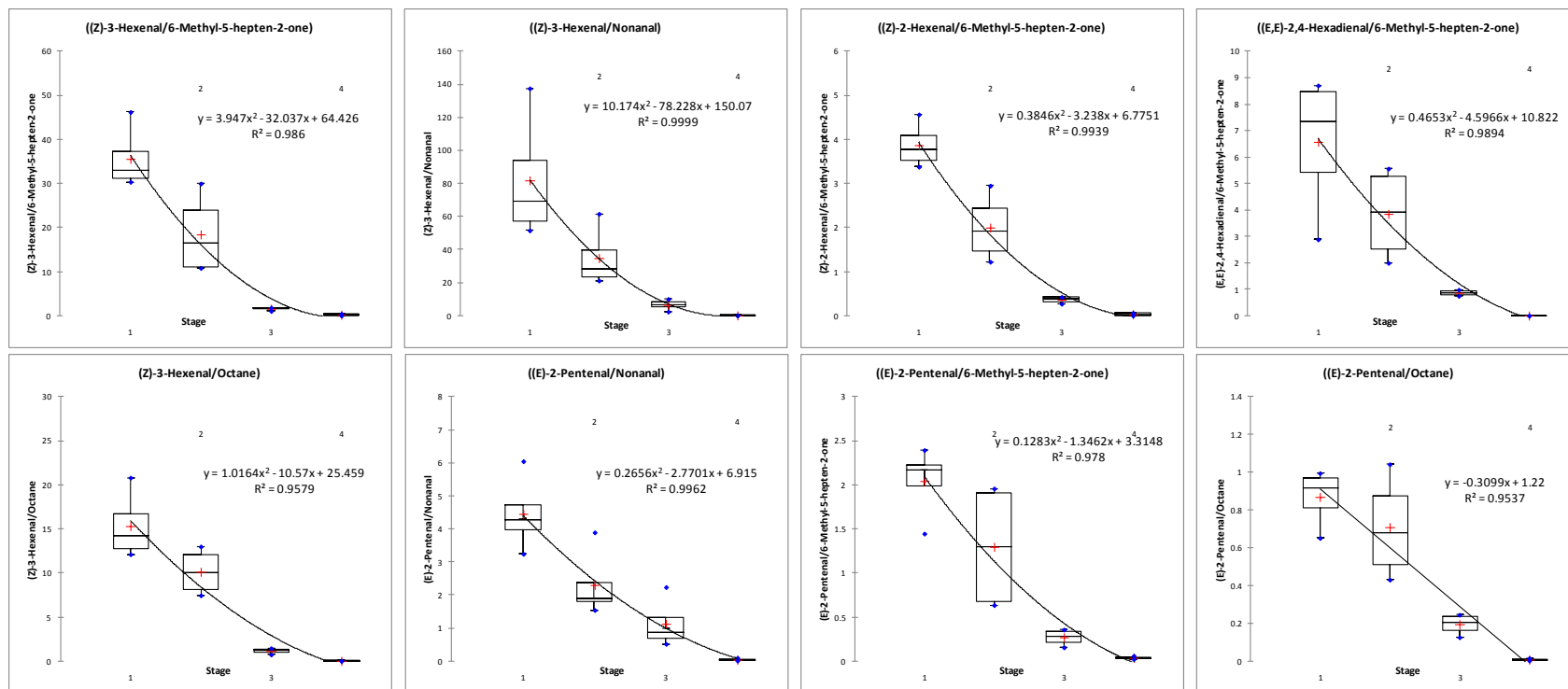


Figure 4

[Click here to download Figure: Figure 4.pptx](#)



**Figure 5**[Click here to download Figure: Figure 5.pptx](#)

**Figure 6**  
[Click here to download Figure: Figure 6.pptx](#)

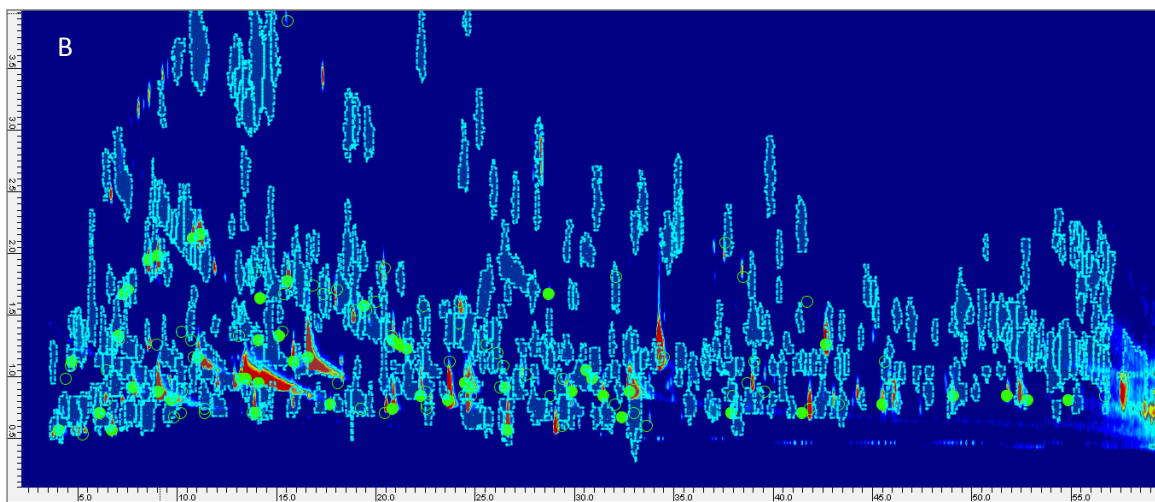
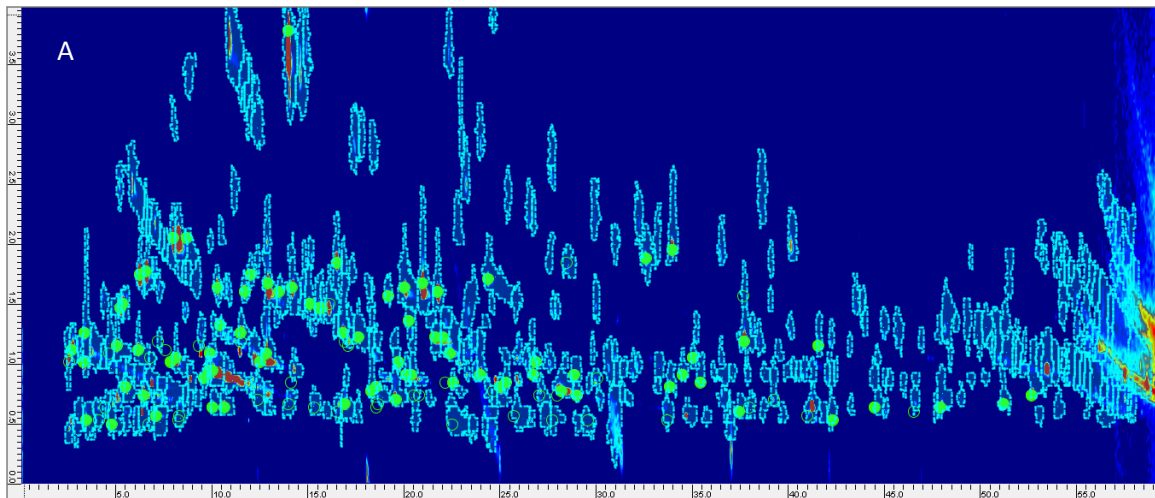
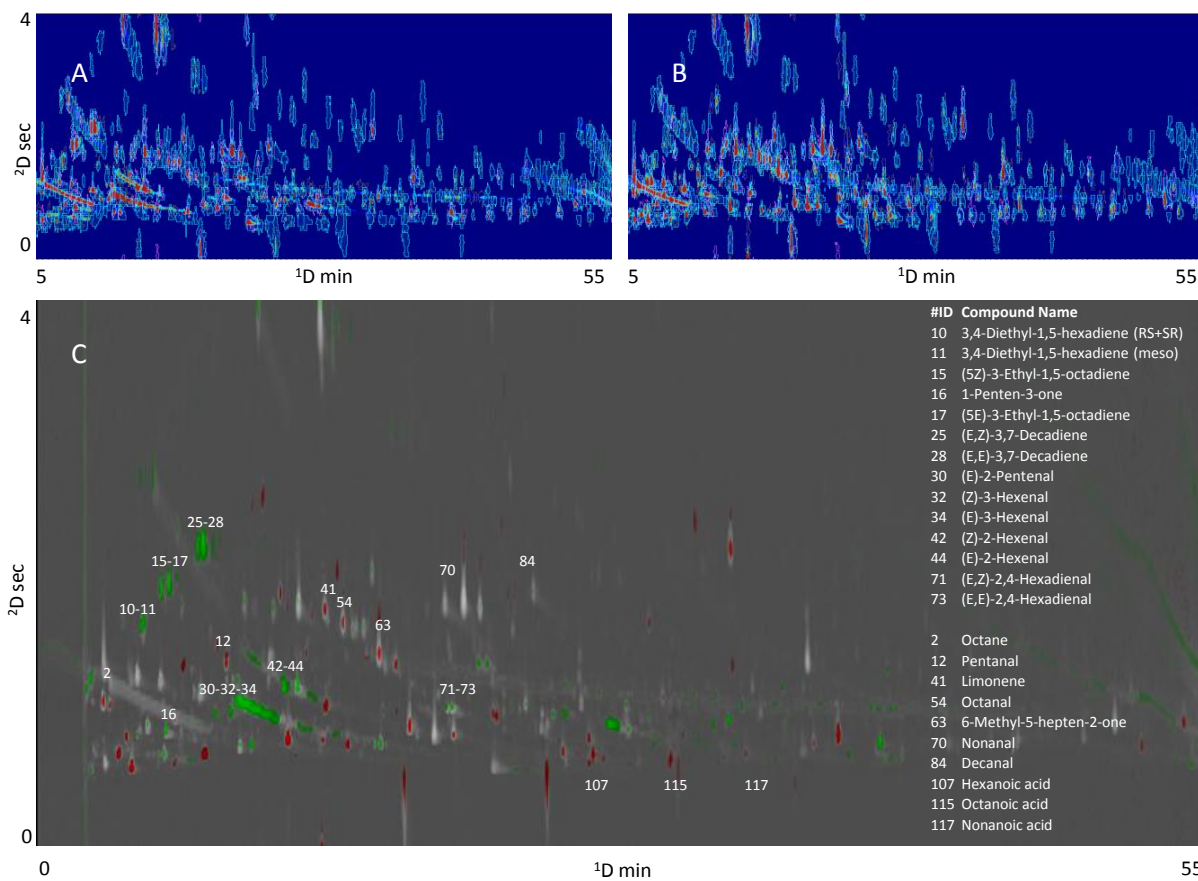




# Figure 7 new

[Click here to download Figure: Figure 7rev.pptx](#)



**Electronic Supplementary Material (online publication only)**

**[Click here to download Electronic Supplementary Material \(online publication only\): Supplementary Table 1.xlsx](#)**

**Electronic Supplementary Material (online publication only)**

**[Click here to download Electronic Supplementary Material \(online publication only\): Supplementary Table 2.xlsx](#)**

**Electronic Supplementary Material (online publication only)**

**[Click here to download Electronic Supplementary Material \(online publication only\): Supplementary Information.pptx](#)**